Journal of the Civil Engineering Forum, September 2022, 8(3): 277-290
DOI 10.22146/jcef.3769
Available Online at: https://journal.ugm.ac.id/v3/JCEF/issue/archive

Chemical Anchor Pullout Force Modeling with Variation of Anchor Embedment Length in Concrete and Concrete Strength

Anis Rosyidah*, Jasun Widiana Putra, Jonathan Saputra
Department of Civil Engineering, Jakarta State Polytechnic, Depok, INDONESIA
Jalan Prof. Dr. G. A. Siwabessy, UI Depok Campus
*Corresponding authors: anis.rosyidah@sipil.pnj.ac.id

SUBMITTED 6 January 2022 **REVISED** 27 April 2022 **ACCEPTED** 2 June 2022

ABSTRACT The embedment length influences the adhesion between the cast iron material and the concrete. The concrete's compression strength also contributes to an increase in bond strength. Therefore, this research aims to determine the maximum pullout force on each variation of the anchor and the optimal embedment length. A gauge is modeled as a rod-type with a diameter of 16 mm, and the embedment lengths used are 5D, 10D, and 15D, while the compressive strengths include f_c' 20, 30, 40, 50, and 60 MPa. Furthermore, a finite element-based application was utilized with the ANSYS Workbench student version. The result showed that the concrete with strengths of 20, 30, 40, 50, and 60 MPa has maximum pullout forces of 27.011, 53.536, 68.657, 68.970, and 84.407 kN, respectively at an embedment length of 15D. It was observed that the failure pattern obtained starts from the defect in the concrete cone and ends with the breakage of reinforcement or steel failure at each variation of concrete strength. A combination of two non-parametric techniques was used in this research, which includes Kruskal Wallis and U-Mann Whitney test. The first technique revealed that the chi-square value for strengths 20, 40, 50, and 60 MPa is 9.486, while that of 30 MPa is 9.881. The second test employed showed a significance value below 0.05. In conclusion, the embedment length affected the value of pullout force, and 15D was the optimum embedment length for each variation of concrete strength. The enhancement in tensile strength increases with the strength of the concrete.

KEYWORDS Maximum Axial Force; Embedment Length; Concrete Strength; Finite Elements; Statistics.

1 INTRODUCTION

Chemical Anchor has been widely used in the construction industry for structural renovation and new construction because of its cost-effectiveness and drying speed (Sibagariang *et al*., 2020). One of the factors affecting the anchor's depth is the bond stress value between the steel and concrete materials. The anchoring of the reinforcing steel works properly when the steel rod is firmly embedded in the concrete at a certain anchorage length, which is usually determined by the reinforcing steel distribution's size (Riani, 2018).

Analytical calculations have not been extensively performed on the anchorage depths, particularly when using adhesives. The practicality factor for determining the anchorage length is prioritized in project implementation by using the standard distance from the anchor factory. Cattaneo and Muciaccia (2016) investigated anchorage implanted with epoxy in high-strength concrete and found that concrete's strength increased when there was an increase in the ultimate tensile load. According to Hu *et al*. (2021), the change in the strength of concrete increased the pullout forces that the anchor is able to withstand. Topcu *et al*. (2016) examined the diameter and depth's effects of chemical anchors and concluded that there was a significant change in the pullout force of the specimen as the depth increased. Upadhyaya and Kumar (2015) found that the adhesive anchorage's load capacity improved linearly with the increasing length of the applied depth and also discovered that the maximum pullout force was most significant at the length of the excellent depth.

Furthermore, Al-fouadi and Mohammed (2018) found that finite element-based tensile technique was currently being used in order to avoid experimental tests that requires more research time and costs. Al-Zuhiri and Sahi (2013) analyzed the bond behavior of reinforcement due to pullout forces on cylindrical concrete and used finite element software to directly compare the results with the

experiment. It was observed that the finite element's results were close to the experimental values. The Ansys software graphically displayed the relationship between load and deflection to prove the theory of failure. This conclusion is consistent with Effendi (2020), which found that the results of the yield stress value in the analyzed material are very close to experimental testing.

Several investigations were conducted on the embedment of these anchors, but most only discussed the use in ordinary concrete strengths, and few did a comparison in different concrete strengths simultaneously (Yilmaz *et al.*, 2013). Therefore, this research aims to provide information about the effect of depth on the anchor's maximum pullout forces and the optimum anchorage length for different concrete strengths. It was observed that the effectiveness of depth distances has a direct impact on the efficiency of materials used and construction costs.

2 METHODS

2.1 Research Flow Design

Chemical anchors and concrete cubes are modeled in Solidwork, which are imported into the Ansys software. Material property data are also included in Ansys for modeling. Afterward, the displacement value of each anchor was inputted and the top of the pedestal was set as fixed support. The final step was to simulate the maximum pullout force and failure model of the anchor or concrete. The data obtained were processed by statistical analysis using the Kruskal Wallis and U-Mann Whitney methods in order to obtain the optimum value of anchor depth for concrete strength. The design of the research flow is shown in Figure 1.

2.2 Research Object

Anchor modeling is considered to be the post-installation method, which was planted in the concrete according to the planned distance and depth. The choice of anchor depth is based on SNI 2847-2019 codes, which range from 5 to 15 times the diameter. The top surface of the concrete pedestal is not allowed to deform i.e. fixed support, and the investigation was conducted by making three depth variations in 5 different concrete models.

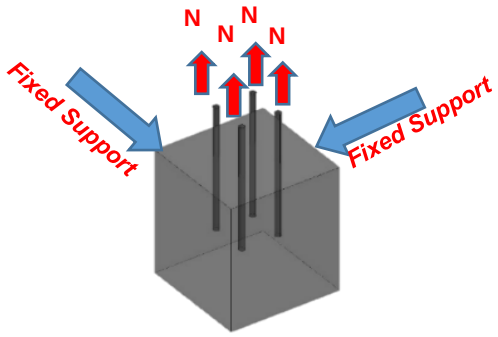

Figure 1. Tensile test modeling on test items

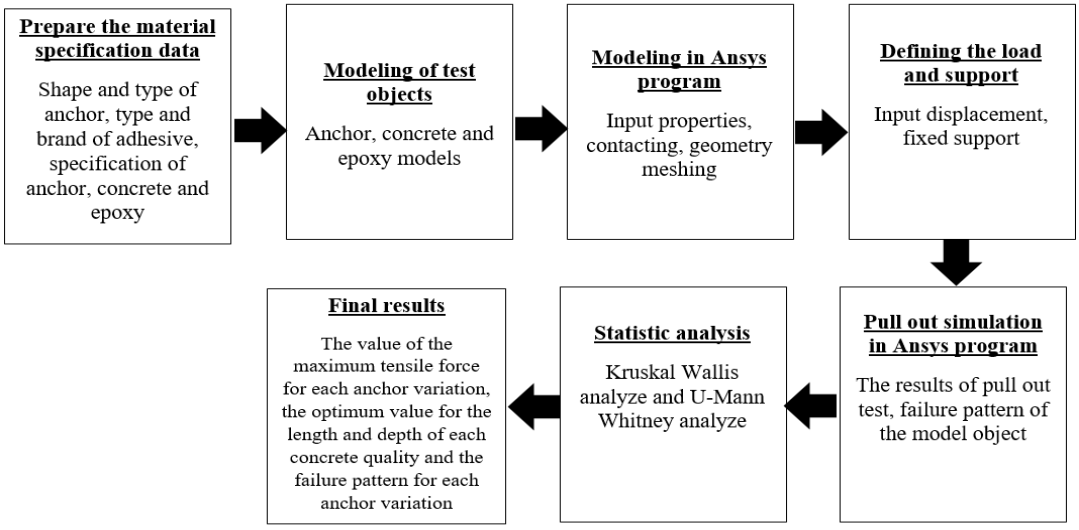

Figure 2. Research design

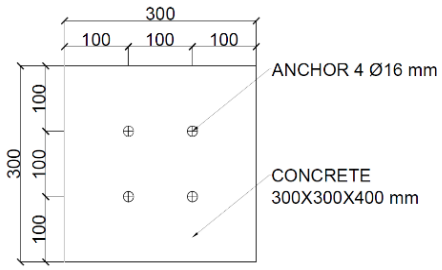

Figure 3. Anchor configuration and installation details

In this research, the three test object models were divided based on the differences in anchor diameter and concrete dimensions, listed in Table 1.

2.3 Object Specification

The model used was the anchor rod Hilti product with M16 diameter and ASTM F568M Grade 5.5 quality. Polyamide (02) 28.08 ALD Epoxy grout was utilized for the adhesive as a chemical anchor. The modeled concrete test object has dimensions for adjusting the anchor depth with different compressive strengths ranging from f'_c 20 MPa, 30 MPa, 40 MPa, 50 MPa, and 60 MPa. Furthermore, the maximum pullout force of concrete strength was obtained by comparing the compressive strength with the pullout forces of the concrete. The average maximum pullout force of low-strength concrete based on SNI 2847-2019 was $0.56\sqrt{f'c}$ compressions, and according to ACI 363R, the concrete's quality was 21-83 MPa using a correlation number of $0.597\sqrt{f'c}$. This SNI 2847-2019 was also used to determine the concrete's modulus of elasticity, and the result showed that for low-strength and normal concretes, $E_c = (W_c)1.5\times0.043\sqrt{f'c}$ and $4700\sqrt{f'c}$, respectively. Meanwhile, for high-strength concrete with the application of ACI 363-92 codes, $E_C = 3320 + 6900\sqrt{f'c}$. Specifically, the strength specifications of the samples to be modeled are summarized in Table 2.

Table 1. Groups and dimensions of the test object model

Anchor Depth (h_{eff})	Concrete Dimensions, w × l × h (mm)				
	A (20 MPa)	B (30 MPa)	C (40 MPa)	D (50 MPa)	E (60 MPa)
5d = 8 mm	300×300×200	300×300×200	300×300×200	300×300×200	300×300×200
10d = 160 mm	300×300×300	300×300×300	300×300×300	300×300×300	300×300×300
15d= 240 mm	300×300×400	300×300×400	300×300×400	300×300×400	300×300×400

Table 2. Specifications of materials used

Material	Density (kg/m³)	Isotropic Elasticity	Strength
Concrete f'_c 20 MPa	2300	Young's Modulus = 21019 MPa Poisson's Ratio = 0.20	Tensile Strength = 2.5 MPa Compressive Strength = 20 MPa
Concrete f'_c 30 MPa	2300	Young's Modulus = 25742 MPa Poisson's Ratio = 0.20	Tensile Strength = 3.26 MPa Compressive Strength = 30 MPa
Concrete f'_c 40 MPa	3000	Young's Modulus = 29725 MPa Poisson's Ratio = 0.20	Tensile Strength = 3.375 MPa Compressive Strength = 40 MPa
Concrete f'_c 50 MPa	3000	Young's Modulus = 30375 MPa Poisson's Ratio = 0.20	Tensile Strength = 4.22 MPa Compressive Strength = 50 MPa
Concrete f'_c 60 MPa	3000	Young's Modulus = 32616 MPa Poisson's Ratio = 0.20	Tensile Strength = 4.48 MPa Compressive Strength = 60 MPa
Anchor	7850	Young's Modulus = 200000 MPa Poisson's Ratio = 0.3	Tensile Yield = 440 MPa Ultimate Tensile = 500 MPa
Polyamide (02) 28.08 ALD Epoxy grout	2000	Young's Modulus = 3300 MPa Poisson's Ratio = 0.3	Pullout forces = 37.68 MPa Compressive Strength = 95 MPa

The specification parameters in Table 2 need to be entered into the Ansys software to match the material's behavior in its original nature for the model to present the mathematical relationship between the load responders (Canonsburg, 2013a).

2.4 Modeling in the Finite Element Software

2.4.1 Geometry and Meshing

In the finite element analysis, the model passed through a meshing stage where it was divided into a series of small elements, and the stresses and strains in these materials were analyzed after loading (Khalaf *et al*., 2020). This stage entails a mixture of volume filling, volume intersection, and volume combination operations that create conformal webs among all solids, fluids, and virtual bodies (Canonsburg, 2013b).

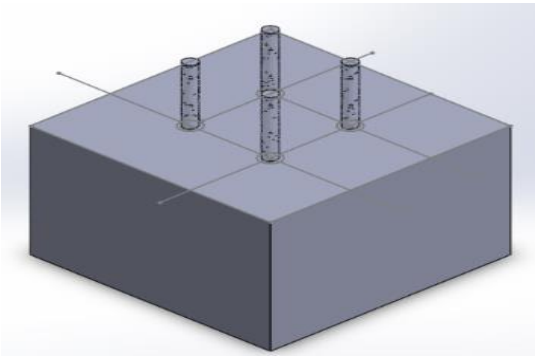

Figure 4. Figure 3D assembly model test object

After the test object model was created in the Solidwork software as shown in Figure 4, it was imported into the student version of Ansys software, in which the meshing was performed. The model was further divided into several small elements with mesh control on each element as shown in Table 3 and Figure 5.

Table 3. Specifications of materials used

Material	Method	Size
Concrete	Tetrahedrons	15 mm
anchor	Tetrahedrons	15 mm
Epoxy	Tetrahedrons	15 mm

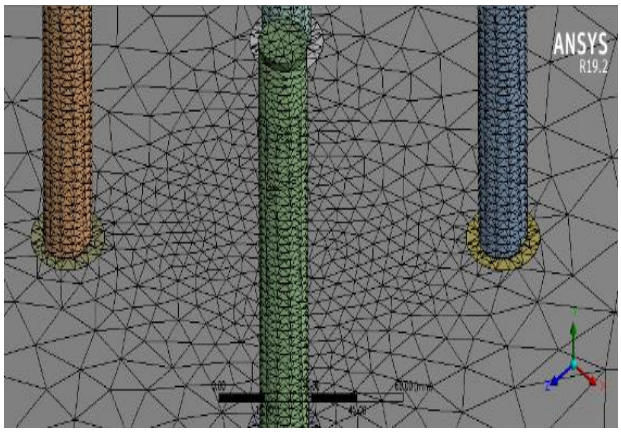

Figure 5. Meshing results of each element

2.4.2 Provision of Contact Pair and Pedestal

The bonded contact type is used for the concrete and the epoxy anchor because the anchor model already has threads, meaning it does not permit friction in the contact. In the process, epoxy portion was used as the bonded contact, while one of the connected elements was applied to a load. The bonding effect begins and becomes more pronounced at the anchorage of the reinforcing ends and around the cracks when stress change occurred in the concrete and steel. Furthermore, the fixed support was selected above the concrete for adjusting the testing conditions. This choice of fixed support eliminated the concrete's deformation and allows the concrete to be stationary and held at the top during loading as shown in Figure 6.

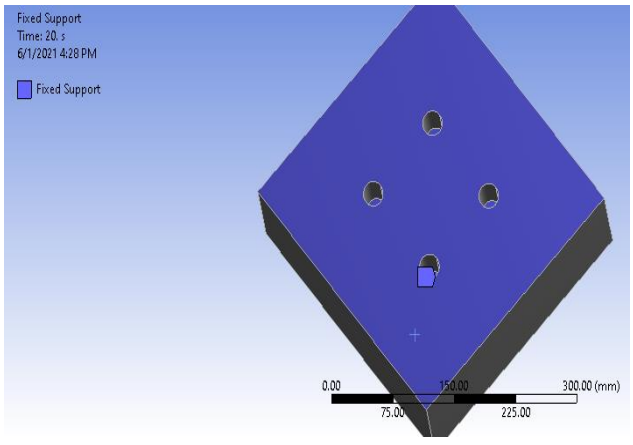

Figure 6. Giving support to the top of the concrete surface

2.4.3 Loading and Solution

Loading was done by entering the respective displacement and time step values of 2.5 cm and 30 into each anchor, as shown in Figure 7. Based on ASTM Standard C.234-919, the test object experienced a pullout failure or detached anchor when the slip value that occurs after loading exceeds 2.5 cm. The maximum pullout force per anchor rod was further determined using the reaction section probe, while the stress on the anchor iron is generated from the axial stress on the Y-axis. The highest primary stress was however applied to the area of the material to present the tensile stress in concrete and epoxy.

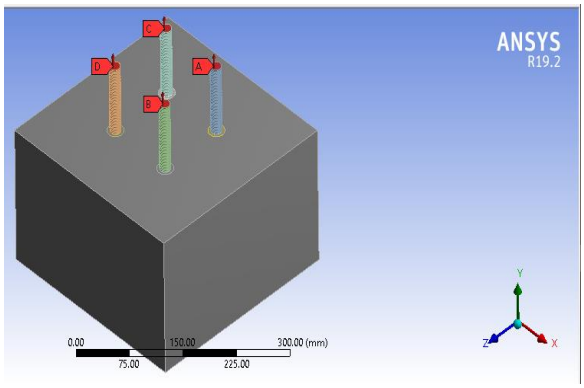

Figure 7. Giving displacement to the top of each anchor

2.5 Non-Parametric Statistical Analysis

Non-parametric statistics, known as assumption-free or distribution-free, are part of the statistical analysis test (Jamco and Balami, 2020). The analysis of each anchor's maximum pullout force was tested using non-parametric statistics with the Kruskal Wallis and the U-Mann Whitney test methods because the amount of data was small and not normally distributed. Consequently, two hypotheses were proposed, namely:

a) H_0: There is no significant difference between depth and the maximum pullout force.
b) H_1: There is a significant difference between the depth effect and the value of maximum pullout force.

2.5.1 Test Kruskal Wallis and U-Mann Whitney

In the Kruskal Wallis test, the hypothesis H_0 is rejected when the calculated chi-square value is > chi-square table, but when the condition is reversed, H_0 is accepted. The values in the chi-square table are based on the degrees of freedom (df) = k−1 and the level of significance (α) (Assegaf *et al.,* 2019). Furthermore, the Mann-Whitney technique was used to test the null hypothesis that there was no significant difference between the two datasets, and that the data were drawn from an irrelevant sample. When the test results reach a significance value below 0.05, H_0 is rejected, and H_1 is accepted (Sriwidadi, 2011).

3 RESULTS

3.1 Relationship between Pullout Forces and Deformation

The slip test was performed with the Ansys Workbench 19.2 program, and the test object model has the same significant displacement value of 2.5 mm with a sub-step of 30. The results are produced by the anchors in each concrete are in the form of slip values with different range of reaction loads, meanwhile every depth produced a different holding force based on the slip value.

According to the test results of the student version of Ansys Workbench program, the average elastic condition of the test object in each concrete has a load value range of 80 to 90 kN. It was observed that the slip value tends to hit and be straightened in the plastic position as the load increases. For example, the slip value at a depth of 10 D in the elastic conditions tend to be smaller than 5D and 15D for concrete strengths of 20 to 40 MPa, meanwhile the slip was not too different for 50 and 60 MPa. This is due to the strength factor of concrete that strongly resist the pullout forces for the anchor to be well restrained.

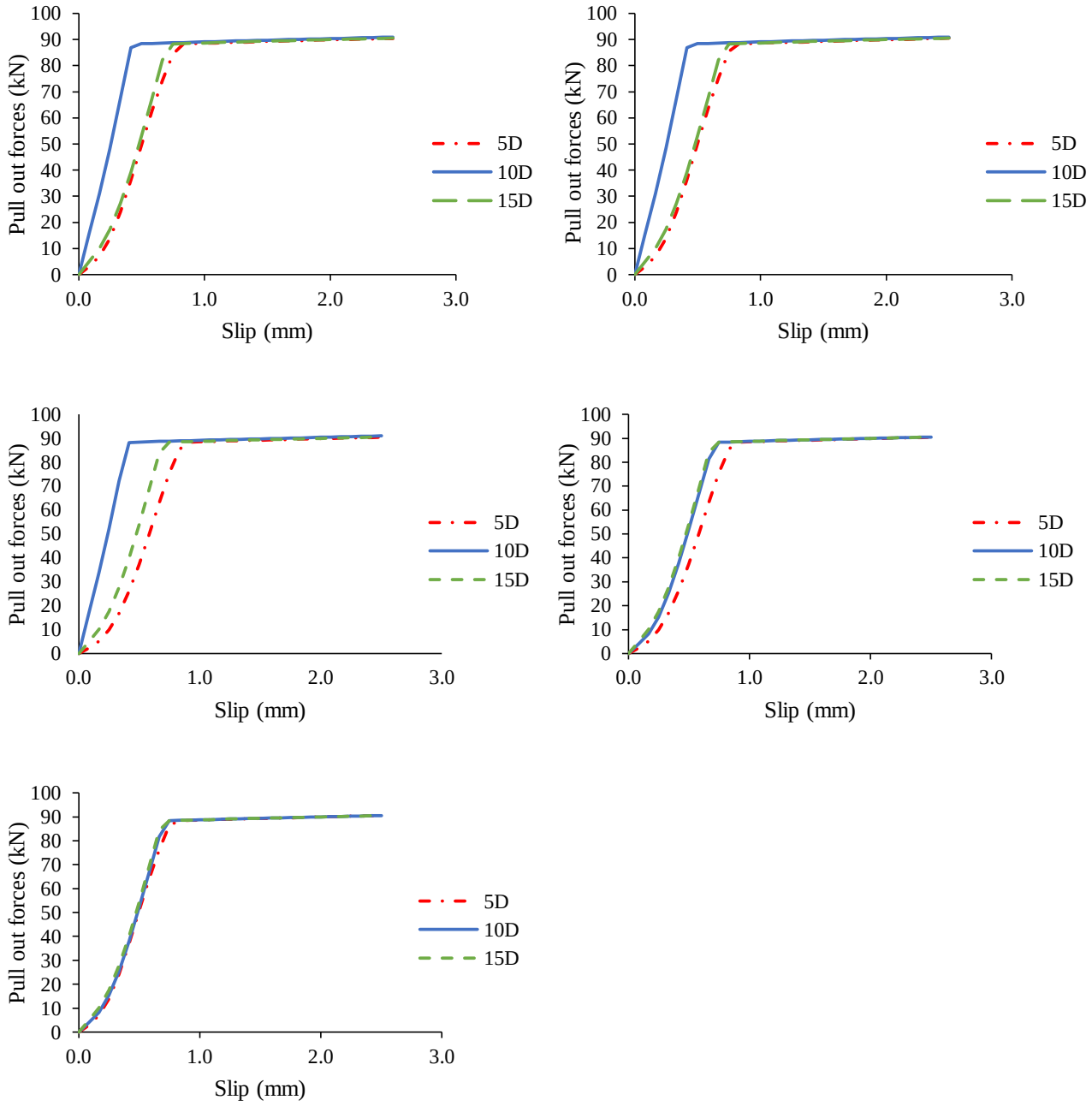

Figure 8. Graph of pullout forces and slip of concrete

3.2 Failure Pattern and Maximum Pullout Forces Value

In this test, the maximum pullout forces value was taken from the state of the test object at the time of the first failure, known as a concrete cone failure, and was presented in Table 4.

3.2.1 Maximum Pullout forces Value and Failure Pattern at 20 MPa Concrete Strength

The maximum pullout forces value of each anchor is in Figure 9. Figure 9 shows that the concrete with strength of 20 MPa has an average maximum pullout forces of 27.201, 13.808, and 15.406 kN at depths of 15, 5, and 10D, respectively. It was observed that the difference between the pullout force values of 5D and 10D was not too much.

3.2.2 Maximum Pullout forces Value and Failure Pattern at 30 MPa Concrete Strength

The maximum pullout forces value of each anchor is in Figure 10. Based on Figure 10, the concrete with strength of 30 MPa has an average maximum pullout force of 53.536 kN at a depth of 15D. It was also observed that the pullout

forces were 13.865 and 32.772 kN at depths of 5D and 10D, respectively.

3.2.3 Maximum Pullout Forces Value and Failure Pattern at 40 MPa Concrete Strength

The maximum pullout forces value of each anchor is in Figure 11. Figure 11 shows that the concrete with strength of 40 MPa has an average maximum pullout force of 53.826 kN at a depth of 15D. It was also observed that at a depth of 5D, the force was 16.840 kN and significantly increased to 33.772 kN at 10D.

3.2.4 Maximum Pullout Forces Value and Failure Pattern at 50 MPa Concrete Strength

The maximum pullout forces value for each anchor is in Figure 12. Figure 12 shows that the concrete with strength of 50 MPa has an average maximum pullout force of 68.970 kN at a depth of 15D. Meanwhile, at depths of 5D and 10D, the forces were 16.893 and 37.883 kN, respectively.

3.2.5 Maximum Pullout Forces Value and Failure Pattern at 60 MPa Concrete Strength

The maximum pullout forces value of each anchor is in Figure 13. According to Figure 13, the concrete with strength of 60 MPa has an average maximum pullout force of 84.407 kN at a depth of 15D. It was also observed that at depths of 5D and 10D, the pullout forces were 24.298 and 52.093 kN, respectively.

Table 4. Maximum pullout forces value on variation of anchor

Concrete Strength (MPa)	No. Anchor	Maximum Pullout Forces (kN) (Cone Concrete Failure)					
		5D	Average	10D	Average	15D	Average
20	A1	13.835	13.808	15.332	15.377	27.215	27.201
	A2	13.834		15.329		27.212	
	A3	13.740		15.431		27.192	
	A4	13.824		15.415		27.185	
30	B1	13.891	13.865	32.817	32.772	53.557	53.536
	B2	13.891		32.838		53.551	
	B3	13.796		32.441		53.516	
	B4	13.881		32.993		53.518	
40	C1	16.856	16.840	33.673	33.772	53.846	53.826
	C2	16.855		33.699		53.841	
	C3	16.805		33.862		53.807	
	C4	16.844		33.852		53.808	
50	D1	16.904	16.888	37.894	37.870	68.998	68.970
	D2	16.903		37.895		68.987	
	D3	16.853		37.806		68.946	
	D4	16.893		37.883		68.949	
60	E1	24.338	24.298	52.123	52.093	84.444	84.407
	E2	24.337		52.124		84.423	
	E3	24.196		52,016		84.374	
	E4	24.322		52.109		84.388	

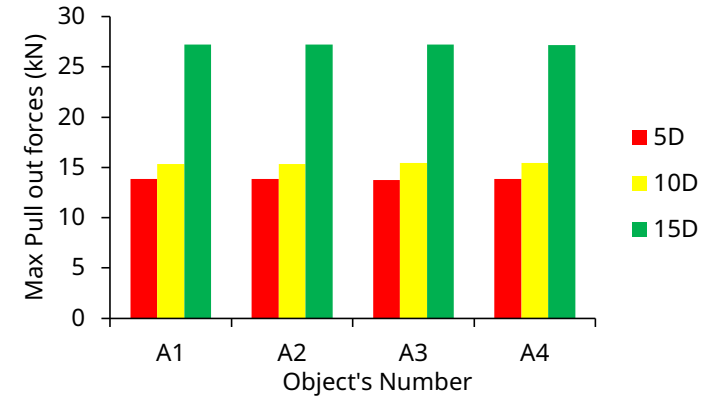

(A)

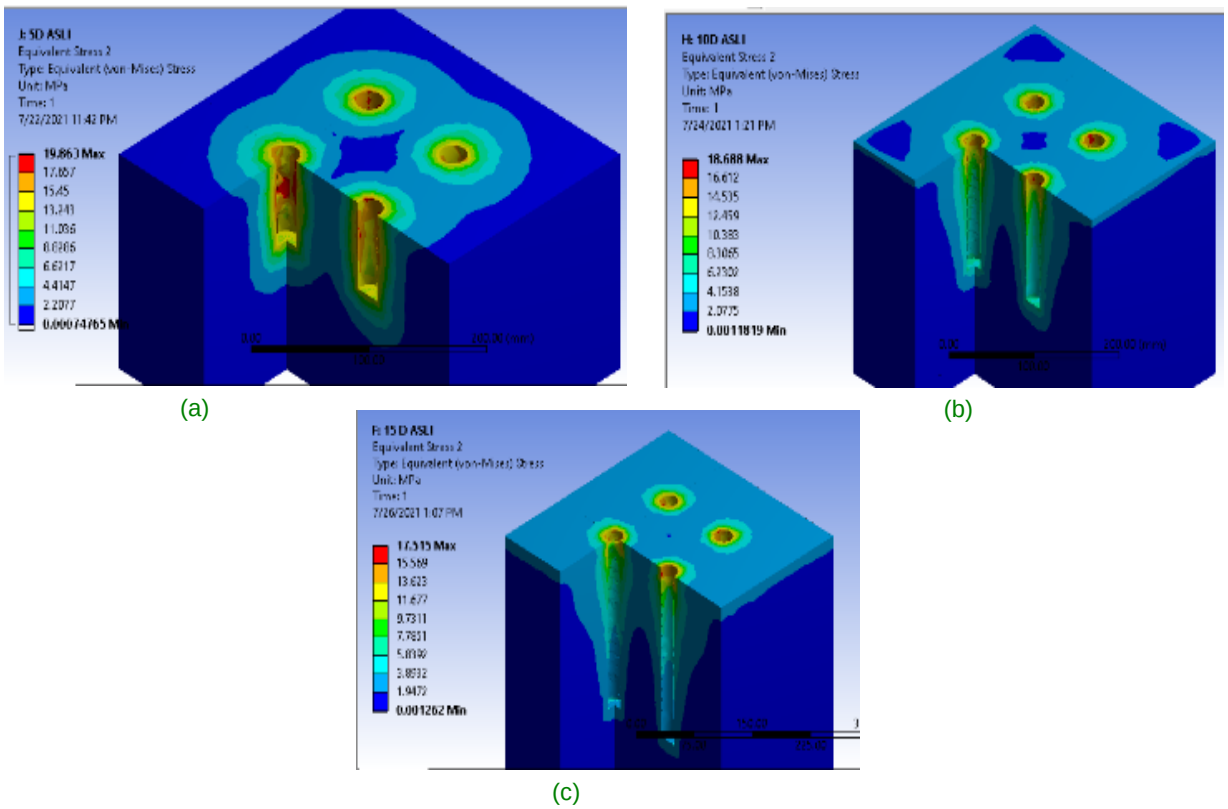

(B)

Figure 9. (A) Diagram of maximum pullout forces value per anchor at 20 MPa concrete strength; (B) The failure pattern of 20 MPa concrete through stress distribution ((a:5D, b:10D, c:15D)

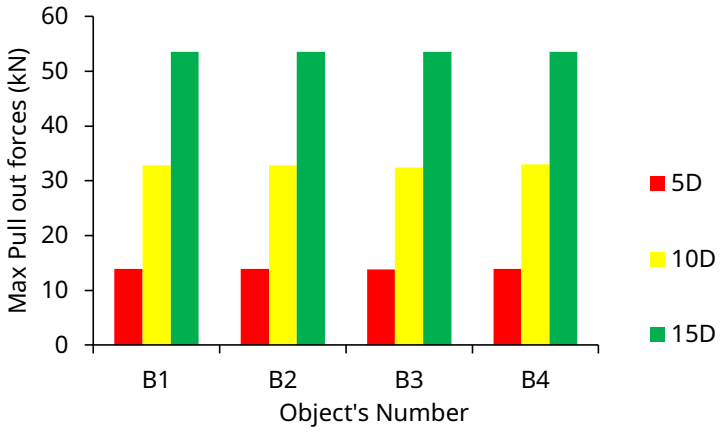

(A)

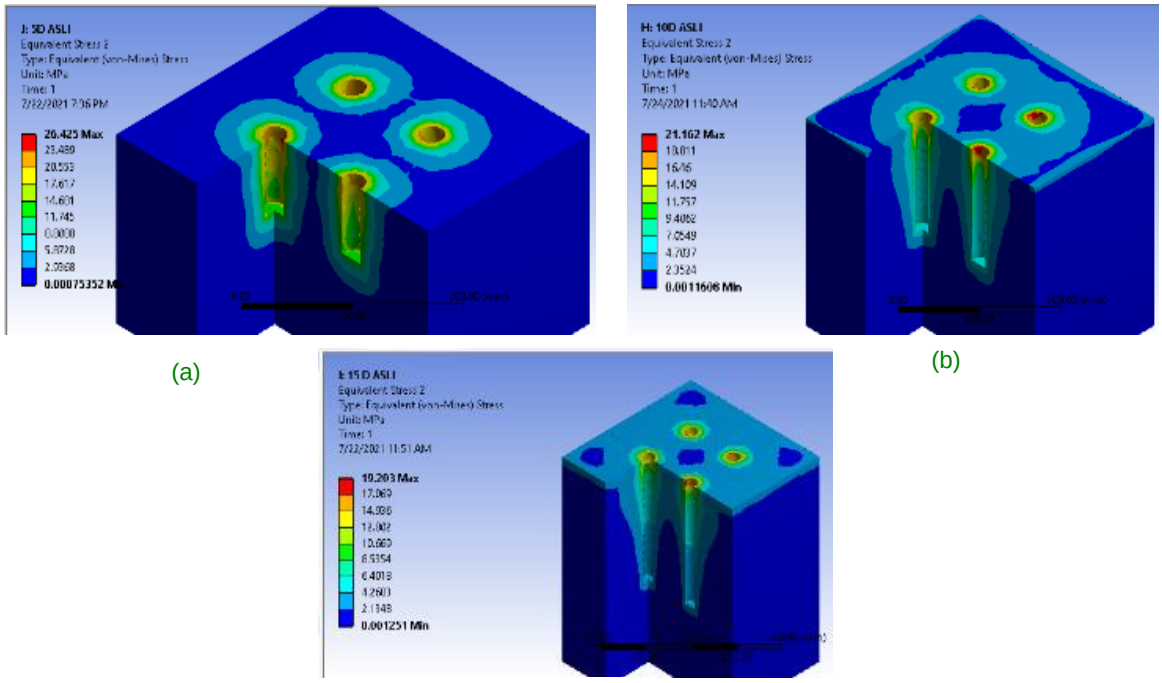

(a) (b)

(c)

(B)

Figure 10. (A) Diagram of maximum pullout forces value per anchor at 30 MPa concrete strength; (B) The failure pattern of 20 MPa concrete through stress distribution ((a:5D, b:10D, c:15D)

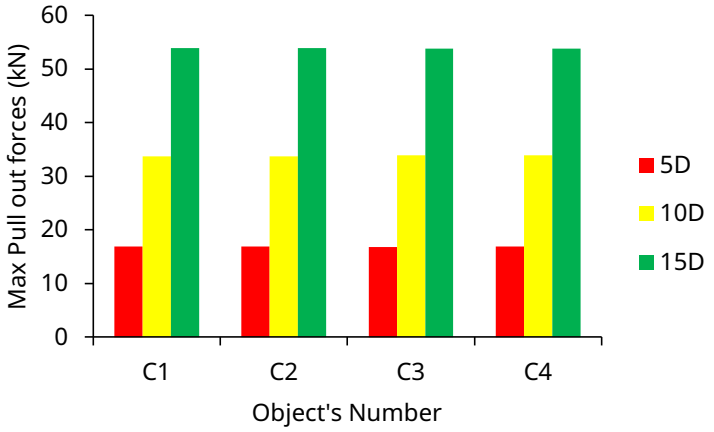

(A)

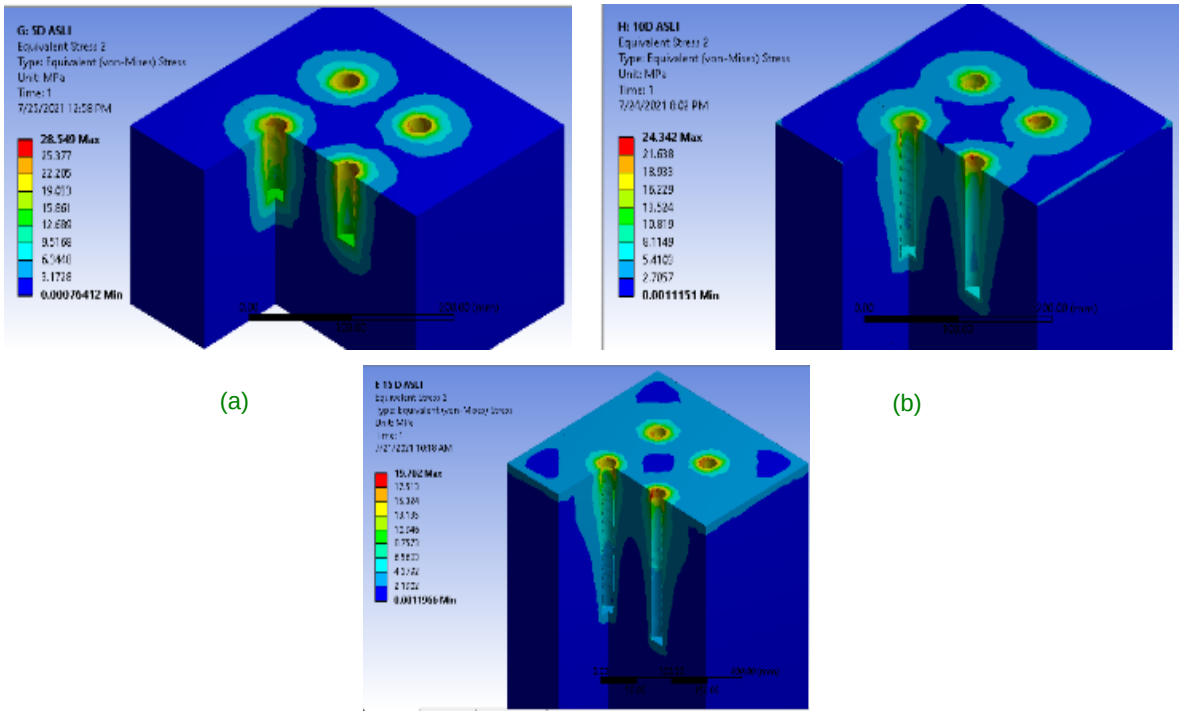

(a) (b)

(c)

(B)

Figure 11. (A) Diagram of maximum pullout forces value per anchor at 40 MPa concrete strength; (B) The failure pattern of 20 MPa concrete through stress distribution ((a:5D, b:10D, c:15D)

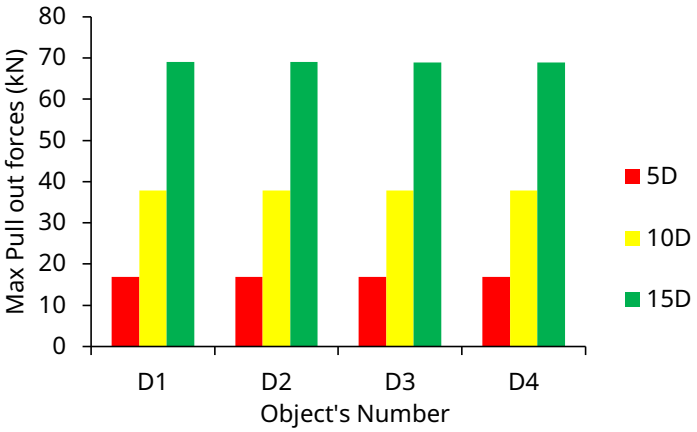

(A)

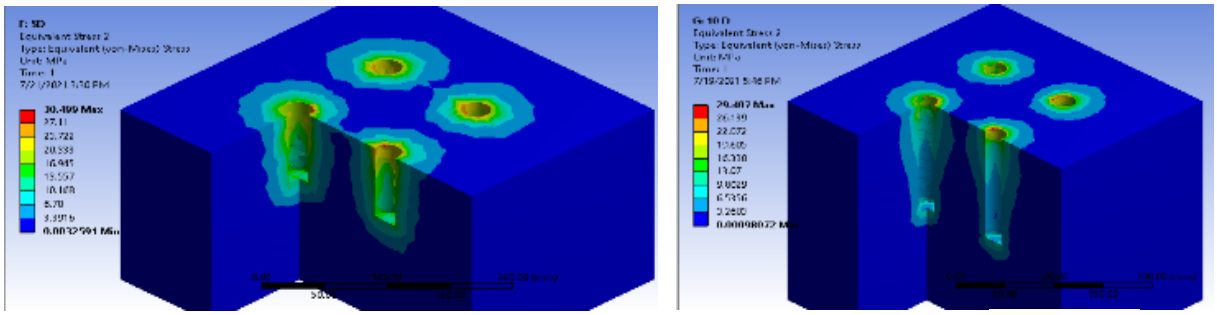

(a)

(b)

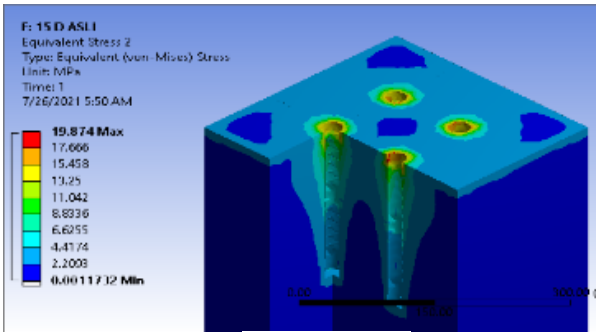

(c)

(B)

Figure 12. (A) Diagram of maximum pullout forces value per anchor at 50 MPa concrete strength; (B) The failure pattern of 20 MPa concrete through stress distribution ((a:5D, b:10D, c:15D)

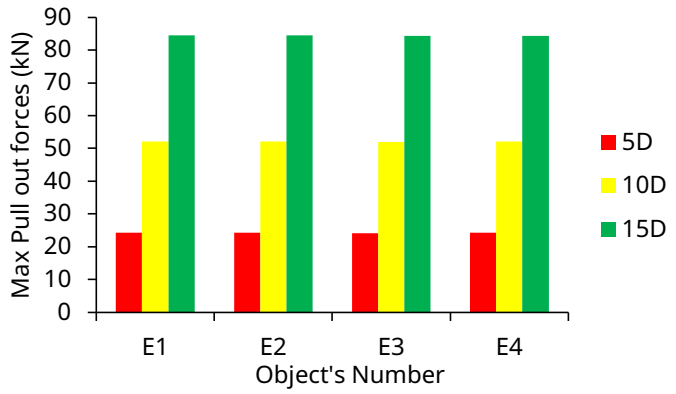

(A)

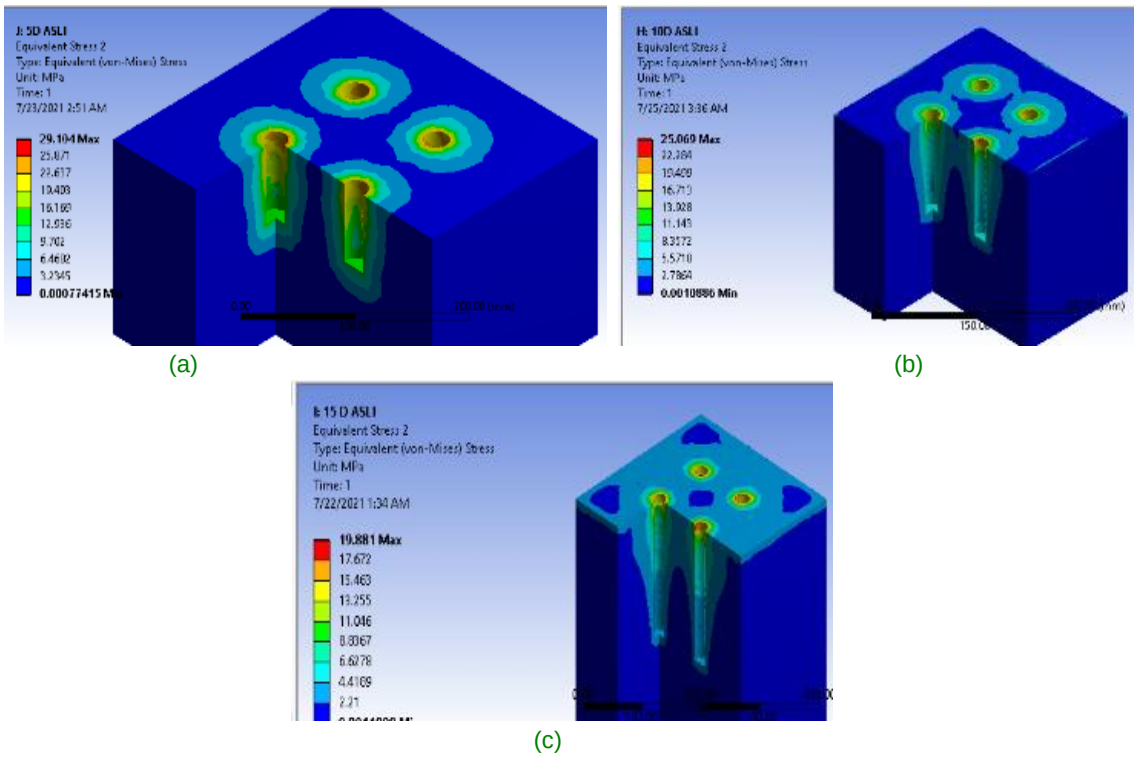

(a) (b)

(c)

(B)

Figure 13. (A) Diagram of maximum pullout forces value per anchor at 60 MPa concrete quality; (B) The failure pattern of 20 MPa concrete through stress distribution ((a:5D, b:10D, c:15D)

3.3 Maximum Pullout Forces Statistical Analysis Results

The Kruskal Wallis technique was used to calculate the size of the significant value from the smallest to the largest. It was observed that when the chi-square value is greater than the chi-square table (5.991), H_0 is rejected, and H_1 is accepted.

Table 5. Kruskal Wallis table of each variation of concrete strength

	Concrete Strength				
	20 MPa	30 MPa	40 MPa	50 MPa	60 MPa
Chi Square	9.846	9.881	9.846	9.846	9.846
df	2	2	2	2	2
Asymp.Sig	0.007	0.007	0.007	0.007	0.007

According to Table 5, the chi-square value for the concrete strengths of 20, 40, 50, and 60 MPa is 9.846, while for 30 MPa, the value is 9.881. It was observed that H_0 is rejected, and H_1 is accepted because the value of all chi-squares is more significant than 5.991. This means the comparison significantly affected the maximum pullout forces between 5D and 15D depth for each concrete quality.

The U-Mann Whitney test was further used to determine the significance value of variations between 5D and 15D as well as 10D and 15D. It was observed that when the test results get a significance value below 0.05, H_0 is rejected, and H_1 is accepted.

Table 6. U-Mann Whitney table of each variation of concrete strength

Value of Sig. Between Depths	Concrete Strength 20 MPa	30 MPa	40 MPa	50 MPa	60 MPa
5D and 15D	0.021	0.021	0.021	0.021	0.021
10D and 15D	0.021	0.021	0.021	0.021	0.021

Based on Table 6, the significance value for each concrete strength is 0.021, and since it is smaller than 0.05, H_0 is rejected, and H_1 is accepted. The two variations comparisons of the length of the 5D and 15D, as well as 10D and 15D showed a significant value, indicating that the optimum embedment length was 15D.

4 DISCUSSION

Based on the results of hypothesis testing, it was discovered that an increase in depth has a significant effect on the maximum tensile force that the anchor is able to withstand. This is consistent with Sibagariang (2020), which concluded that the variation in different embedment lengths affected the pullout strength retained on each anchor. This means that the increase in the length of the anchor embedment leads to higher maximum tensile force. Furthermore, Topcu *et al*. (2016) discussed the effect of the diameter and embedment of chemical anchors, and found a significant change in the pullout strength capacity of the test object as the embedment length increased. Upadhyaya and Kumar (2015) also concluded that the load capacity of anchors with adhesives increased linearly with an increase in the length of the embedment.

5 CONCLUSION

The results showed that the failure pattern in this test generally starts from the defect of the concrete cone for all concrete strengths. Meanwhile, it was observed from the results of hypothesis testing that an increase in the embedment significantly affected the maximum pullout force that the anchor was able to withstand, and the optimum embedment length was 15D. This means that as the strength of the concrete increased, the maximum pullout force resisted was greater. This is supported by Breitenbucher *et al*. (2014), which examined the behavior of the maximum pullout forces of steel fiber in different variations of concrete strength, and found that the increase in tensile resistance is generally influenced by the strength of the concrete.

DISCLAIMER

The authors declare no conflict of interest.

ACKNOWLEDGMENTS

The author is grateful to UP2M Politeknik Negeri Jakarta, which has assisted in this research.

REFERENCES

Al-fouadi, WKA, and Mohammed, AH (2018) "Experimental and analytical study on the behavior of pullout failure of reinforcing bar embedded in concrete blocks," Structural Concrete, 20(July), pp. 171–184.

Al-Zuhairi, A. and Sahi, W. (2013) "Numerical prediction of bond-slip behavior in simple pullout concrete specimens," University of Baghdad Engineering Journal, 19(1), pp. 1–12.

Assegaf, A., Mukid, MA, and Hoyyi, A. (2019) "Analysis of Bank Health Using Local Mean K-Nearest Neighbor and Multi Local Means K-Harmonic Nearest Neighbor," Gaussian Journal,

8(3), pp. 343–355.

Breitenbucher, R. et al. (2014) "Experimental, analytical and numerical analysis of the pullout behavior of steel fibers considering different fiber types, inclinations, and concrete strengths," Structural Concrete, 15(2), pp. 126–135.

Canonsburg, TD (2013a) ANSYS Mechanical APDL Material Reference. Canonsburg, PA 15317.

Canonsburg, TD (2013b) ANSYS Meshing User's Guide. Canonsburg, PA.

Cattaneo, S. and Muciaccia, G. (2016) "Adhesive anchors in high-performance concrete," Materials and Structures/Materiaux et Constructions, 49(7), pp. 2689–2700.

Effendi, MK (2020) "Non-Linear Finite Element Analysis of Flexural Reinforced Concrete Beam using Embedded Reinforcement Modeling," Journal of the Civil Engineering Forum, 6(3), p. 271.

Hu, Z., Shah, YI and Yao, P. (2021) "Experimental and numerical study on interface bond strength and anchorage performance of steel bars within prefabricated concrete," Materials, 14(13).

Jamco, juan charles and Balami, abdul malik (2020) "Kruskal-Wallis analysis to determine student learning concentration based on the field of interest of the Unpatti Fmipa Statistics Study Software," Journal of Mathematics, Statistics, and Applied Research, 1(1), pp. 39–44.

Khalaf, RD et al. (2020) "Analytical Study on Effect of Bar Size on Pull-out force for Reinforcing Bar Embedded in Concrete Blocks," IOP Conference Series: Materials Science and Engineering, 928(2).

Prayogo, GM, Rosyidah, A. and Ketut Sucita, I. (2018) "Modeling of the Reinforcement Minimum Spacing of Precast Concrete Using Grouting," Proceedings - 2018 International Conference on Applied Science and Technology, iCAST 2018, pp. 674–679.

Riani, E. (2018) The Effect of Anchoring Depth Variations on Bond Strength of Deformed Steel Reinforcements in Normal Concrete, Lightweight Concrete and High Quality Concrete. Mataram University.

Sibagariang, Y. et al. (2020) Experimental study of anchor pull out forces with variations in distance, Juitech. Quality University.

Sriwidadi, T. (2011) "Using the Mann-Whitney Test on the Analysis of the Effect of Salesperson Training on New Product Sales," Binus Business Review, 2(2), p. 751.

Topcu, IB et al. (2016) "Prediction of Pullout Performance of Chemical Anchors Embedded into Concrete," ICENS, 24-28, pp. 440–457.

Upadhyaya, P. and Kumar, S. (2015) "Pullout capacity of adhesive anchors: An analytical solution," International Journal of Adhesion and Adhesives, 60, pp. 54–62.

Yilmaz, S., zen, MA and Yardim, Y. (2013) "Tensile behavior of post-installed chemical anchors embedded to low strength concrete," Construction and Building Materials, 47, pp. 861–866. doi:10.1016/j.conbuildmat.2013.05.032.